A flavin-dependent monooxygenase produces nitrogenous tomato aroma volatiles using cysteine as a nitrogen source

David K. Liscombe[a,b,1], Yusuke Kamiyoshihara[c,1,2], Jérémie Ghironzi[d], Christine J. Kempthorne[a,e], Kevin Hooton[a], Blandine Bulot[d], Vassili Kanellis[f], James McNulty[f], Nghi B. Lam[c], Louis Félix Nadeau[d], Michael Pautler[g], Denise M. Tieman[c], Harry J. Klee[c,3], and Charles Goulet[d,3]

[a]Biochemistry Group, Vineland Research and Innovation Centre, Vineland Station, ON LOR 2E0, Canada; [b]Department of Biological Sciences, Brock University, St. Catharines, ON L2S 3A1, Canada; [c]Horticultural Sciences, University of Florida, Gainesville, FL 32611; [d]Département de Phytologie, Université Laval, Quebec City, QC G1V 0A6, Canada; [e]Chemical Biotechnology Graduate Program, Brock University, St. Catharines, ON L2S 3A1, Canada; [f]Department of Chemistry and Chemical Biology, McMaster University, Hamilton, ON L8S 4M1, Canada; and [g]Genomics Services, Platform Genetics Inc., Vineland Station, ON L0R 2E0, Canada

Contributed by Harry J. Klee; received October 11, 2021; accepted December 17, 2021; reviewed by Mark Lange and Sarah O'Connor

Tomato (*Solanum lycopersicum*) produces a wide range of volatile chemicals during fruit ripening, generating a distinct aroma and contributing to the overall flavor. Among these volatiles are several aromatic and aliphatic nitrogen-containing compounds for which the biosynthetic pathways are not known. While nitrogenous volatiles are abundant in tomato fruit, their content in fruits of the closely related species of the tomato clade is highly variable. For example, the green-fruited species *Solanum pennellii* are nearly devoid, while the red-fruited species *S. lycopersicum* and *Solanum pimpinellifolium* accumulate high amounts. Using an introgression population derived from *S. pennellii*, we identified a locus essential for the production of all the detectable nitrogenous volatiles in tomato fruit. Silencing of the underlying gene (*SlTNH1*;*Solyc12g013690*) in transgenic plants abolished production of aliphatic and aromatic nitrogenous volatiles in ripe fruit, and metabolomic analysis of these fruit revealed the accumulation of 2-isobutyl-tetrahydrothiazolidine-4-carboxylic acid, a known conjugate of cysteine and 3-methylbutanal. Biosynthetic incorporation of stable isotope-labeled precursors into 2-isobutylthiazole and 2-phenylacetonitrile confirmed that cysteine provides the nitrogen atom for all nitrogenous volatiles in tomato fruit. *Nicotiana benthamiana* plants expressing SlTNH1 readily transformed synthetic 2-substituted tetrahydrothiazolidine-4-carboxylic acid substrates into a mixture of the corresponding 2-substituted oxime, nitro, and nitrile volatiles. Distinct from other known flavin-dependent monooxygenase enzymes in plants, this tetrahydrothiazolidine-4-carboxylic acid *N*-hydroxylase catalyzes sequential hydroxylations. Elucidation of this pathway is a major step forward in understanding and ultimately improving tomato flavor quality.

aroma volatile biosynthesis | *N*-hydroxylation | organosulfur metabolism | flavor chemistry

Tomato (*Solanum lycopersicum*) is the most valuable fruit and vegetable crop produced worldwide. Intensive breeding programs over the last half century have emphasized traits that are important to producers such as yield, disease resistance, appearance, and postharvest shelf life (1). While those traits are important, modern commercial cultivars tend to fall short of the flavor potential demonstrated by older inbred varieties (2), in part due to lack of tools to breed for aroma profiles that appeal to consumers (3). A systematic approach to identify the most important chemicals contributing to consumer preferences, their biosynthetic pathways, and the genes regulating their synthesis provides essential information for improving flavor (2–5).

Tomato fruit volatiles are synthesized from multiple precursors that include fatty acids, carotenoids, as well as aromatic and aliphatic amino acids. Most of these precursors are essential nutrients for animals, suggesting that volatiles could serve as cues for the presence of important nutrients within the fruit (6). Essential amino acids are metabolically linked to multiple tomato volatiles that are important determinants of consumer perception and preference. For example, phenylalanine is converted to 2-phenylacetaldehyde and 2-phenylethanol (7) while valine, leucine, and isoleucine are linked to isobutanal/ol, 3-methylbutanal/ol, and 2-methylbutanal/ol, respectively (8). Volatiles have essential roles in plants including, defense responses against herbivores and pathogens, plant-to-plant interactions, and attraction of pollinators and seed dispersers (9–11). Thus, the unique volatile profile of each species is likely a result of the adaptation and evolution of each species to their environment.

Tomato fruits also produce nitrogen-containing volatiles that are relatively uncommon in fruits, including 2-phenylacetonitrile (benzyl cyanide), 1-nitro-2-phenylethane, 3-methylbutanenitrile (isovaleronitrile), 1-nitro-3-methylbutane, and 2-isobutylthiazole (Fig. 1*A*) (12). Emissions of aliphatic and aromatic aldoximes,

Significance

Aroma is an important factor in consumer perception and acceptance of fresh tomatoes and involves a cocktail of several dozen compounds. Tomato fruits produce uncommon nitrogen-containing volatiles derived mainly from the amino acids leucine and phenylalanine. These volatiles have strong positive correlations with consumer liking. We show that an enzyme active in ripening tomatoes is responsible for the production of all nitrogenous volatiles in tomato fruit, at the expense of substrates derived from cysteine and volatile aldehydes. This discovery defines a cysteine-dependent route to nitrogenous volatiles in plants, prompting a reconsideration of the impact of sulfur metabolism on tomato flavor and quality.

Author contributions: D.K.L., Y.K., H.J.K., and C.G. designed research; D.K.L., Y.K., J.G., C.J.K., K.H., B.B., N.B.L., L.F.N., D.M.T., and C.G. performed research; D.K.L., V.K., J.M., and M.P. contributed new reagents/analytic tools; D.K.L., Y.K., J.G., C.J.K., K.H., B.B., V.K., J.M., and C.G. analyzed data; and D.K.L., Y.K., H.J.K., and C.G. wrote the paper.

Reviewers: M.L., Washington State University; S.O., Max Planck Institute for Chemical Ecology.

The authors declare no competing interest.

[1]D.K.L. and Y.K. contributed equally to this work.

[2]Present address: College of Bioresource Sciences and Graduate School of Bioresource Sciences, Nihon University, Fujisawa, Kanagawa, 252-0880, Japan.

[3]To whom correspondence may be addressed. Email: charles.goulet@fsaa.ulaval.ca or hjklee@ufl.edu.

This article contains supporting information online at http://www.pnas.org/lookup/suppl/doi:10.1073/pnas.2118676119/-/DCSupplemental.

Published February 7, 2022.

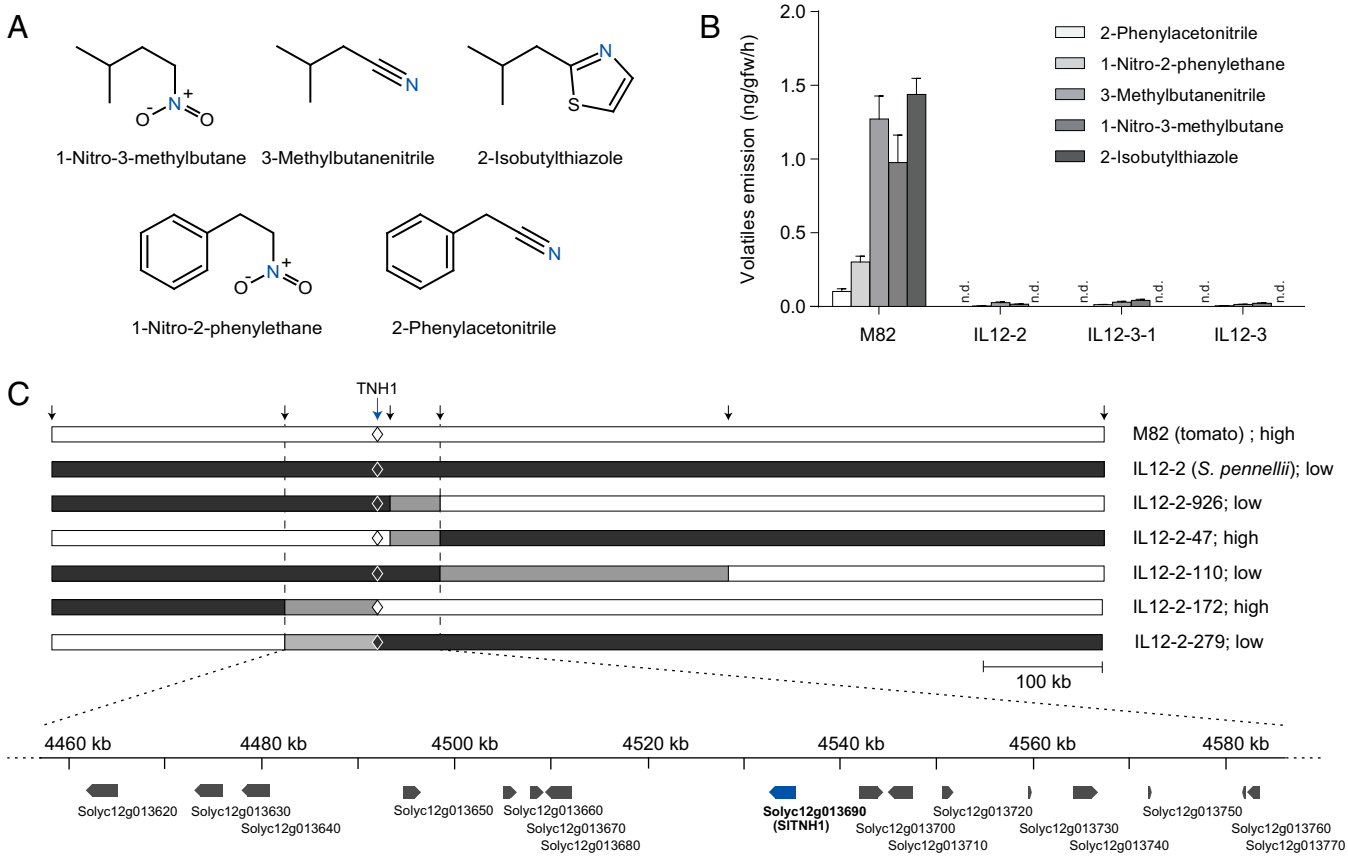

Fig. 1. A gene on Chr12 (Solyc12g013690) is responsible for nitrogenous volatiles biosynthesis in tomato fruit. (*A*) Structures of main nitrogenous volatiles detected in tomato fruit. (*B*) Emissions of nitrogenous volatiles from cut ripe fruits of ILs and the tomato parent, cv. M82 (±SE, $n = 6$). The amount of each nitrogenous volatile is significantly different between M82 and the ILs ($P < 0.01$). n.d., not detectable. (*C*) Fine mapping of a nitrogenous volatile-related QTL on chromosome 12. A set of recombinants with low or high (wild type) content of nitrogenous volatiles was derived from a cross between M82 and IL12-2. The illustration shows a small segment of chromosome 12 where the QTL is located. White and dark-gray sections represent genomic segments from *S. lycopersicum* and *S. pennellii*, respectively. Arrows indicate the positions of markers used to define recombinants. The light-gray sections represent the regions where a recombination occurred, as delimited by molecular markers. The color inside the diamonds indicates whether the ILs contain the *S. lycopersicum* (white) or *S. pennellii* (dark-gray) version of Solyc12g013690. The QTL region as defined by volatile content is shown by dashed lines and enlarged below to show details (assembly SL2.50).

nitriles, and nitro compounds have been observed from herbivore-damaged and pathogen-infected plants (13–16). In damaged leaves of *Populus*, 2-phenylacetonitrile and aliphatic aldoximes have important roles in recruiting parasitic insects (17), while phenylacetaldoxime appears to be involved in direct defense against herbivores (18). A parallel can be drawn with the tomato that needs to recruit frugivores to disperse its seeds. Given that the production of nitrogenous volatiles is specific to the ripe fruit, the nitrogenous volatiles likely serve the purpose of making the fruit more attractive to seed dispersers.

Although nitrogenous volatiles tend to have pungent, medicinal odors at higher concentrations, they can impart desirable flavor qualities at lower concentrations as part of volatile blends. For example, 2-phenylacetonitrile and 1-nitro-2-phenylethane have floral odors, and the latter has long been considered to be a notable contributor to tomato flavor (19, 20). Consumer preference panels conducted with a large set of tomato varieties indicated that several of the nitrogenous volatiles positively correlate with consumer liking (5). While nitrogenous volatiles are important for tomato flavor, they are largely absent from fruits of other species, with melon being one of the few exceptions (21). In contrast, nitrogenous volatiles are relatively common constituents of floral volatile blends (22–25) and are known to be produced in the herbivore-damaged leaves of some plants (9, 16). The biosynthesis of nitrogenous volatiles in other plants implicate CYP79 enzymes that utilize amine substrates (26). In melon, it appears there may be two routes to the formation of 2-phenylacetonitrile (21).

Despite the importance of the nitrogenous volatiles to tomato flavor, their biosynthesis has not been elucidated in this species. It was previously shown that tomato aromatic amino acid decarboxylases (AADCs) catalyze the conversion of phenylalanine to 2-phenylethylamine, the precursor of 2-phenylacetaldehyde and 2-phenylethanol (7). Ripe fruits of transgenic tomatoes overexpressing *AADC*s have higher emission of not only 2-phenylacetaldehyde and 2-phenylethanol, but also 1-nitro-2-phenylethane and 2-phenylacetonitrile, indicating that those aromatic nitrogenous volatiles share part of the same pathway. However, empirical evidence is lacking regarding the pathway for synthesis of aliphatic nitrogenous volatiles. Based on structural considerations, 3-methylbutanenitrile, 1-nitro-3-methylbutane, and 2-isobutylthiazole are most likely leucine derivatives (27).

A powerful strategy to identify the genes involved in volatile synthesis is to exploit natural variation within the genus. Thus, populations of introgression lines (ILs) that contain defined segments of chromosomes from the wild relatives of tomato have been used to identify numerous volatile-associated quantitative trait loci (QTLs) (12, 27, 28). These QTLs, in turn, permit identification of genes that define the synthetic pathway as well as points of regulation (29–31). Here we utilized a

Solanum pennellii IL population to identify a QTL responsible for biosynthesis of nitrogenous volatiles. Following fine mapping, we identified a gene encoding a flavin-dependent monooxygenase (FMO) that plays an essential role in aliphatic and aromatic nitrogenous volatile production in tomato fruit and uses 2-substituted thiazolidines derived from cysteine as substrates.

Results

An Essential Gene for Nitrogenous Volatile Production. A *S. pennellii* IL population (28) was screened for QTLs affecting the synthesis of nitrogenous volatiles in ripe fruit. Among these lines, IL12-2, IL12-3-1, and IL12-3, exhibited significant reductions in nitrogenous volatiles (Fig. 1*A*) relative to the tomato parental background (cultivar [cv.] M82) (Fig. 1*B*). The three ILs all contain an overlapping segment of *S. pennellii* chromosome 12 (*SI Appendix*, Fig. S1), so an F_2 population derived from a cross between IL12-2 and M82 was screened for recombination events for more precise mapping of the locus. The new recombinants obtained were fixed (homozygous) in a subsequent generation to give a new set of smaller ILs. The volatile profile of each line was measured for fine mapping of the nitrogenous volatile QTL (Fig. 1*C*) permitting us to localize the QTL to an ∼100-kb region predicted to contain 16 genes (solgenomics.net). Among these, *Solyc12g013690* was selected for further analysis since it was annotated as a "monooxygenase FAD-binding protein" and was therefore considered the best candidate from a biochemical perspective. We examined *Solyc12g013690* expression in IL12-2, IL12-3, IL12-3-1, and the *S. pennellii* parent (LA0716) using primers targeting a consensus region between the *S. lycopersicum* and *S. pennellii* alleles. Compared with control M82, the ILs and *S. pennellii* had very low expression in ripe fruits (*SI Appendix*, Fig. S1). The reduction in the transcript level of *Solyc12g013690* was hypothesized to be the cause of the substantially lower levels of nitrogenous volatiles in the ILs.

The function of Solyc12g013690 and its putative role in nitrogenous volatile production was assessed by antisense-mediated suppression of gene expression in transgenic tomatoes (cv. Large Red Cherry). The volatile contents of ripe fruits from over 20 independent transgenic lines had consistently lower nitrogenous volatile contents. Four independent lines with substantial reductions in *Solyc12g013690* transcript levels were further analyzed (Fig. 2*A*). Significant reductions of nitrogenous volatiles were observed for all four lines compared to the control (Fig. 2*B* and *SI Appendix*, Table S1). Contents of related phenylalanine- and leucine-derived alcohols and aldehydes were not affected in the transgenic lines, indicating that the gene impacts mostly nitrogenous volatiles (*SI Appendix*, Table S1).

We measured the contents of 2-phenylacetonitrile, 1-nitro-2-phenylethane, 3-methylbutanenitrile, 1-nitro-3-methylbutane, and 2-isobutylthiazole in tomato fruits at different stages to determine whether their accumulation is also coupled to the ripening process, like many other flavor volatiles (12). The five major nitrogenous volatiles in cultivar M82 were below the level of detection before the onset of ripening, but substantially increased during ripening (Fig. 3*A*). Quantitative PCR analysis showed that expression of *Solyc12g013690* in fruit is elevated at the initiation of ripening and reaches a maximum level at the fully ripe stage (Fig. 3*B*), consistent with the pattern of nitrogenous volatile production. Leaves and flowers exhibit substantially lower *Solyc12g013690* expression. Since ripening-related gene expression is often regulated by ethylene, the hormone responsiveness of *Solyc12g013690* was tested. Ethylene treatment at the mature green stage resulted in elevated expression in wild-type (WT) fruits (cv. Pearson). This increase was greatly attenuated in *Never-ripe* (*Nr*; cv. Pearson background), an ethylene-insensitive mutant (Fig. 3*C*) (32). Treatment of ripe fruits with 1-methylcyclopropene (1-MCP), a potent inhibitor of ethylene perception (33), reduced *Solyc12g013690* expression (Fig. 3*C*). This ethylene responsiveness indicates that nitrogenous volatile production is ethylene dependent in tomato fruits.

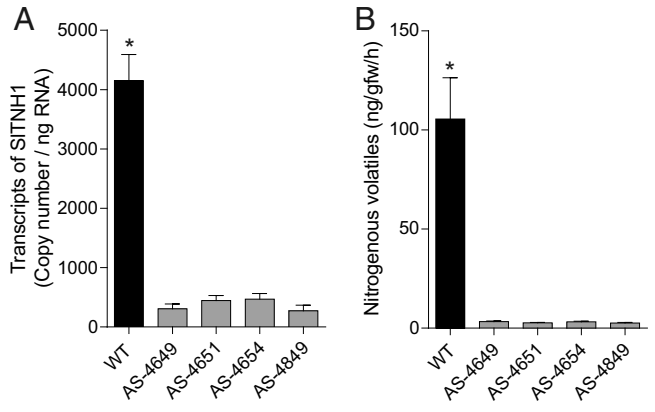

Fig. 2. Antisense-mediated silencing of Solyc12g013690 (*SlTNH1*) results in significant reductions in nitrogenous flavor volatiles in fruit. (*A*) Transcript levels in fruits of four independent transgenic antisense lines relative to the control, cv. Large Red Cherry (±SE, $n = 4$). The transgenic lines were all significantly different from the control (*$P < 0.01$). (*B*) Sum of the emissions of detected nitrogenous volatiles from cut ripe fruits of control and the transgenic lines (±SE, $n = 4$) (*$P < 0.01$) (see *SI Appendix*, Table S1 for emission of each individual compound).

A New Type of FMO in Plants. A phylogenetic analysis using amino acid sequences of tomato and *Arabidopsis* FMOs was performed to determine the relationship of Solyc12g013690 to functionally characterized FMOs (*SI Appendix*, Fig. S2). Solyc12g013690 does not cluster with any enzymes of known function and is distantly related to FMO enzymes in clades I, II, and III, which were previously defined by Schlaich (34). Rather, Solyc12g013690 is more closely related to zeaxanthin epoxidases (ZEPs, clade IV) and squalene epoxidases (SQEs, clade V), clearly defining a distinct clade (clade VI) (*SI Appendix*, Fig. S2). Notably, *Solyc12g013690* transcripts are abundant in ripe fruit compared to other members of this clade (*SI Appendix*, Table S2). FMO enzymes can also be classified based on their fold and function (35). Clades I, II, and III all belong to group B with two α/β Rossmann-like domains for binding FAD and NAD(P)H. Members of clades IV to VII have instead a glutathione reductase (GR-2)-type Rossmann fold and belong to groups A and E. Clades IV and V are classified as group E members because of their epoxidase activities. Based on their homology to bacterial FMOs, clade VI members likely belong to group A and are predicted to perform a hydroxylation. There are two highly conserved FAD-binding motifs in group A enzymes, "GxGxxG" for the adenosine diphosphate (ADP) moiety (36) and "GD" for the riboflavin moiety (37), located at the N-terminal region (11 to 16 amino acids [aa]) and the center of the sequence (294 to 295 aa), respectively (*SI Appendix*, Fig. S3). In addition, a "DG fingerprint" motif occurs in all group A members. That motif, associated with binding of both FAD and NAD(P)H (37), also occurs near the center of the sequences (157 to 158 aa). We examined the newly defined clade VI members for conserved amino acids (*SI Appendix*, Fig. S3). All members of clade VI in *Arabidopsis*, tomato, soybean, poplar, and maize, contain two Leu residues adjacent to the FAD-binding motif, giving "GxGxxGLxxxxL." Also, near the N terminus, there is a highly conserved "VLxxxxxRxxG" sequence. Finally, all members of clade VI have a "RG" motif between the DG and GD fingerprint motifs.

PLANT BIOLOGY

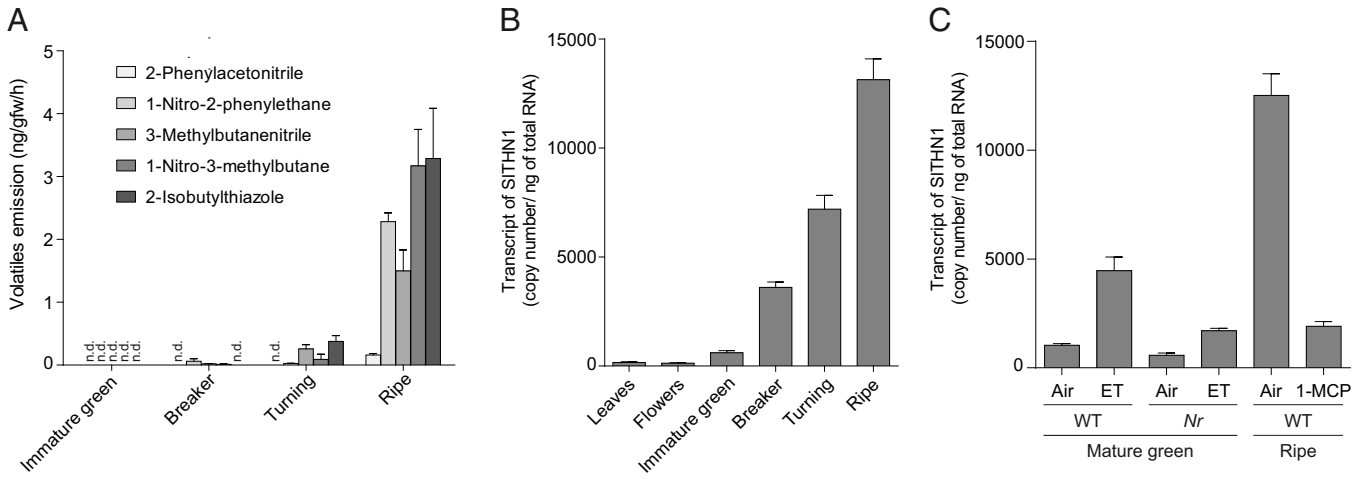

Fig. 3. Ripening-related accumulation of nitrogenous volatiles and Solyc12g013690 (*SlTNH1*) expression in tomato. (*A*) Emissions of nitrogenous volatiles from cut fruits of cv. M82 during the ripening process (±SE, $n = 4$). n.d., not detectable. (*B*) Solyc12g013690 transcript levels in leaves, flowers, and throughout the fruit ripening (immature green, breaker, turning, and ripe) of tomato cv. M82 (±SE, $n = 4$). (*C*) Solyc12g013690 transcript level in response to ethylene (ET) (±SE, $n = 3$). Mature green fruits of cv. Pearson and Never-ripe were treated with ethylene for 16 h. Alternatively, fruits at ripe stage were treated with the inhibitor of ethylene perception, 1-MCP, for 12 h.

Gene Silencing Leads to Accumulation of a Sulfurous Substrate. Our initial attempts to functionally express *Solyc12g013690* focused on assays using primary amine substrates (i.e., 2-phenethylamine), based on current models for volatile biosynthesis in tomato (38). We were unable to demonstrate activity using any amine substrates, so we turned to a nontargeted metabolomics approach using plants with impaired *Solyc12g013690* expression to facilitate identification of potential substrates (34). Antisense-mediated suppression of *Solyc12g013690* expression in tomatoes leads to near-complete abolishment of nitrogenous volatile production (Fig. 2*B* and *SI Appendix*, Table S1), which we anticipated would also result in the accumulation of pathway precursors, including acceptable substrates for the enzyme encoded by *Solyc12g013690*. Nontargeted ultra performance liquid chromatography quadrupole time-of-flight mass spectrometry (UPLC-QTOF-MS) profiling of ripe fruit and comparison of metabolite profiles of *Solyc12g013690*-silenced lines (Fig. 4*C*) versus the unsilenced control using orthogonal projections to latent structures discriminant analysis (OPLS-DA) (*SI Appendix*, Fig. S4) revealed a mass spectral feature, "5.40_190.0896m/z" that consistently accumulated in antisense lines (Fig. 4*B*). Moreover, an ethylmethane sulfonate (EMS)-induced stop-codon variant line (W278*) we isolated contains significantly higher levels of this metabolic feature compared to WT background (Fig. 4*B* and *SI Appendix*, Table S3). Assuming that the empirical *m/z* represents the protonated pseudomolecular ion, this exact mass most likely corresponds to the molecular formula $C_8H_{15}NO_2S$ (−3.02 ppm mass error), which is consistent with the known biological metabolite *S*-prenylcysteine. This compound appeared to be a reasonable candidate substrate for Solyc12g013690, as there is precedence for FMO enzymes that metabolize prenylated cysteines in plants (39). However, following additional experimentation and review of our results and published literature in this context, we could not reconcile how *S*-prenylcysteine could be a substrate for Solyc12g013690, so we considered other possible structural isomers that we may have missed. One such compound is a cyclic analog of *S*-prenylcysteine, 2-isobutyltetrahydrothiazolidine-4-carboxylic acid (IT4C) (Fig. 4*A*), a compound previously documented in the flavor chemistry literature in the context of brewing science (40). We synthesized IT4C from L-cysteine and 3-methylbutanal according to Ershov et al. (41), and verified the structure by proton NMR analysis (*SI Appendix*, Fig. S5). The synthetic IT4C standard coeluted with the feature 5.40_190.0896m/z that accumulates under suppression of *Solyc12g013690* expression when analyzed by UPLC-QTOF-MS (Fig. 4*C*), and the retention time, exact mass, and fragmentation pattern of this mass spectral feature from tomato fruit match those of synthetic IT4C, confirming the identity of this metabolite. Therefore, several complementary samples indicate that IT4C is a likely substrate of Solyc12g013690, which implicates cysteine as the nitrogen source for nitrogenous volatiles. Moreover, we identified another mass spectral feature that disappeared with the abolishment of Solyc12g013690 activity, representing a potential product of the enzyme. The mass spectral data for this feature are consistent with a glutathione conjugate of 3-methylbutanal oxime (*SI Appendix*, Fig. S6), analogous to spontaneous glutathione conjugates formed from *N*-hydroxylated precursors in glucosinolate biosynthesis (42), supporting an *N*-hydroxylating role for Solyc12g013690.

Cysteine Provides the Nitrogen Atom for Nitrogenous Volatiles. To investigate the origin of the nitrogen atom in the biosynthesis of nitrogenous volatiles, we fed ^{15}N, $^{13}C_3$-L-cysteine, and/or ^{15}N,$^{13}C_6$-L-leucine to breaker-stage tomatoes growing on the vine in the greenhouse, and volatiles were collected from those fruit at the red ripe stage. Atmospheric pressure gas chromatography (APGC)-QTOF-MS was used to analyze fruit volatile contents. Interrogation of the 2-isobutylthiazole peak at 5.7 min (*SI Appendix*, Fig. S7) showed a clear mass shift of +8 (*m/z* 150) for the protonated pseudomolecular ion of 2-isobutylthiazole (unlabeled M+H is *m/z* 142) (*SI Appendix*, Fig. S7 *D* and *E*), corresponding to ^{15}N,$^{13}C_7$-2-isobutylthiazole, which represented 0.2% of the total isobutylthiazole (Fig. 5). Feeding labeled leucine alone resulted in 2.5% isotopic enrichment of 2-isobutylthiazole. Labeled leucine contributes +5 mass units to 2-isobutylthiazole (*SI Appendix*, Fig. S7*B*), corresponding to labeling of C2 and the 2-isobutyl moiety but not the nitrogen. Nearly 5% isotopic enrichment of 2-isobutylthiazole was observed with feeding of ^{15}N,$^{13}C_3$-L-cysteine on its own (Fig. 5), which resulted in a mass shift of +3 for the protonated pseudomolecular ion (*m/z* 145), indicating that cysteine contributes the C2N unit of the thiazole ring (*SI Appendix*, Fig. S7*C*). Furthermore, we confirmed that the nitrogen does not originate from the amino acid donor that provides the R group at the 2 position, by feeding ^{15}N,$^{13}C_9$-Phe to

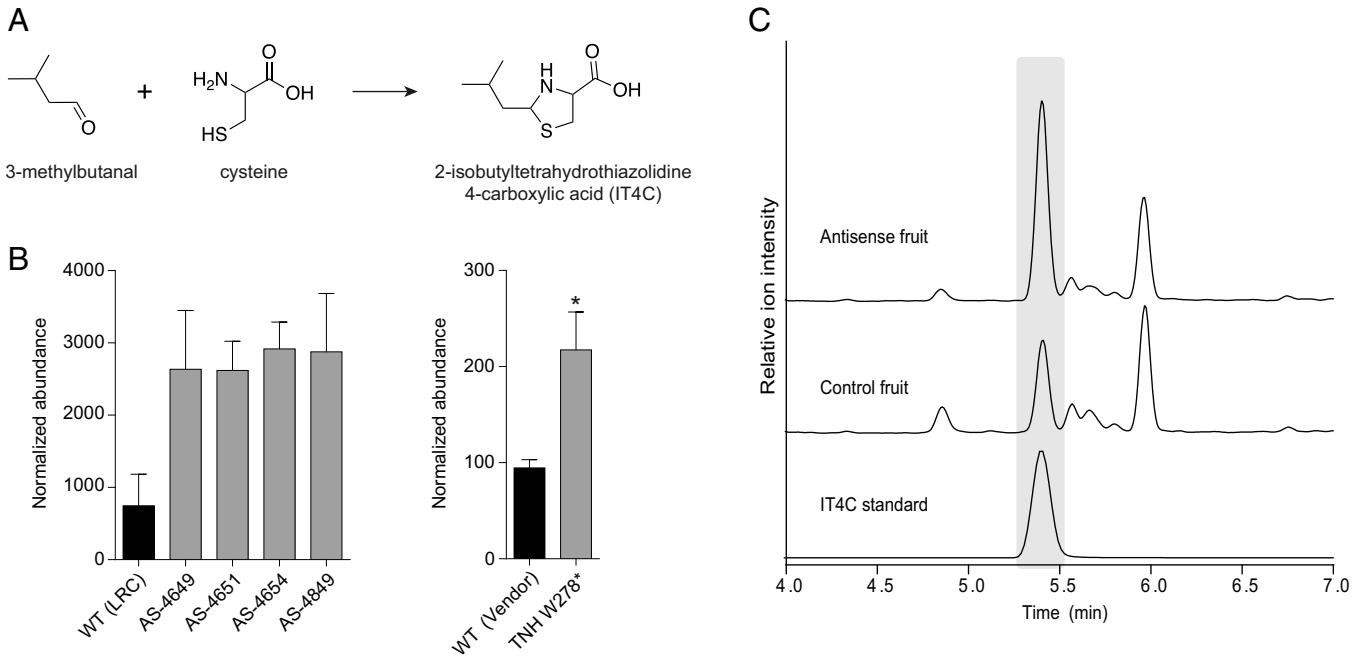

Fig. 4. Impairment of SlTNH1 activity leads to accumulation of 2-isobutyltetrahydrothiazolidine-4-carboxylic acid (IT4C) in tomato fruit. (*A*) IT4C can be easily synthesized from L-Cys and 3-methylbutanal. (*B*) Untargeted metabolomics by UPLC-QTOF-MS revealed that IT4C accumulates in the *SlTNH1* antisense lines and stop codon variant ($n = 3$, ±SE, $*P < 0.05$). (*C*) Extracted ion chromatogram for *m/z* 190.0902 shows that the metabolic feature accumulating in *SlTNH1* antisense lines was unambiguously identified as IT4C. Synthetic IT4C coelutes with the same feature in tomato fruit. MS/MS and NMR spectra of IT4C are provided in the *SI Appendix*.

another set of tomatoes. We found 2-phenylacetonitrile is labeled, but a mass shift of M+8 (*m/z* 125) rather than M+9 (*m/z* 126) indicated that all atoms except for the labeled carboxyl carbon (lost via AADC-mediated decarboxylation) and the labeled nitrogen were incorporated intact (*SI Appendix*, Fig. S8). These results suggest that cysteine provides the nitrogen for all nitrogenous volatiles in tomato fruit and provide further support for 2-substituted thiazolidines as natural products in tomato and the native substrates for the enzyme encoded by *Solyc12g013690*.

Tetrahydrothiazolidine *N*-Hydroxylase. The *Solyc12g013690* cDNA was transiently expressed in *Nicotiana benthamiana* leaves to characterize the catalytic activity of the encoded enzyme. We synthesized 2-substituted thiazolidine substrates according the Ershov et al. (41), specifically those derived from L-Cys (Fig. 4*A* and *SI Appendix*, Fig. S5) or D-Cys and 3-methylbutanal, and L-Cys and 2-phenylacetaldehyde (*SI Appendix*, Fig. S10). *N. benthamiana* leaves producing recombinant Solyc12g013690 produced significantly more 3-methylbutanenitrile, 3-methylbutylaldoxime, 1-nitro-3-methyl-butane, and 2-isobutylthiazole

	Isotopolog	Incorporation ratio ± SEM, %	Position of the labeled carbons and nitrogen in 2-isobutylthiazole
Precursor feeding			
L-Cysteine- $^{13}C_3$,^{15}N	M+3	4.7 ± 2.0	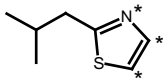
L-Leucine- $^{13}C_6$,^{15}N	M+5	2.5 ± 0.7	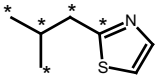
L-Leucine- $^{13}C_6$,^{15}N + L-Cysteine- $^{13}C_3$,^{15}N	M+8	0.2 ± 0.02	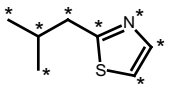

Fig. 5. Biosynthetic incorporation of stable isotope-labeled cysteine and leucine into 2-isobutylthiazole when fed in situ to Tomatoes-on-the-vine at the orange stage. Incorporation ratios were calculated from peak integration areas (PIAs) from APGC-MS/MS analysis where incorporation ratio = [(PIA isotopolog)/(PIA unlabeled + PIA isotopolog) × 100]. $n \geq 3$ for all treatments. Expected *m/z* for 2-isobutylthiazole [M+H] (unlabeled) = 142.0690, [M+H+3] isotopolog = 145.0728, [M+H+5] isotopolog = 147.0856, and [M+H+8] isotopolog = 150.0896.

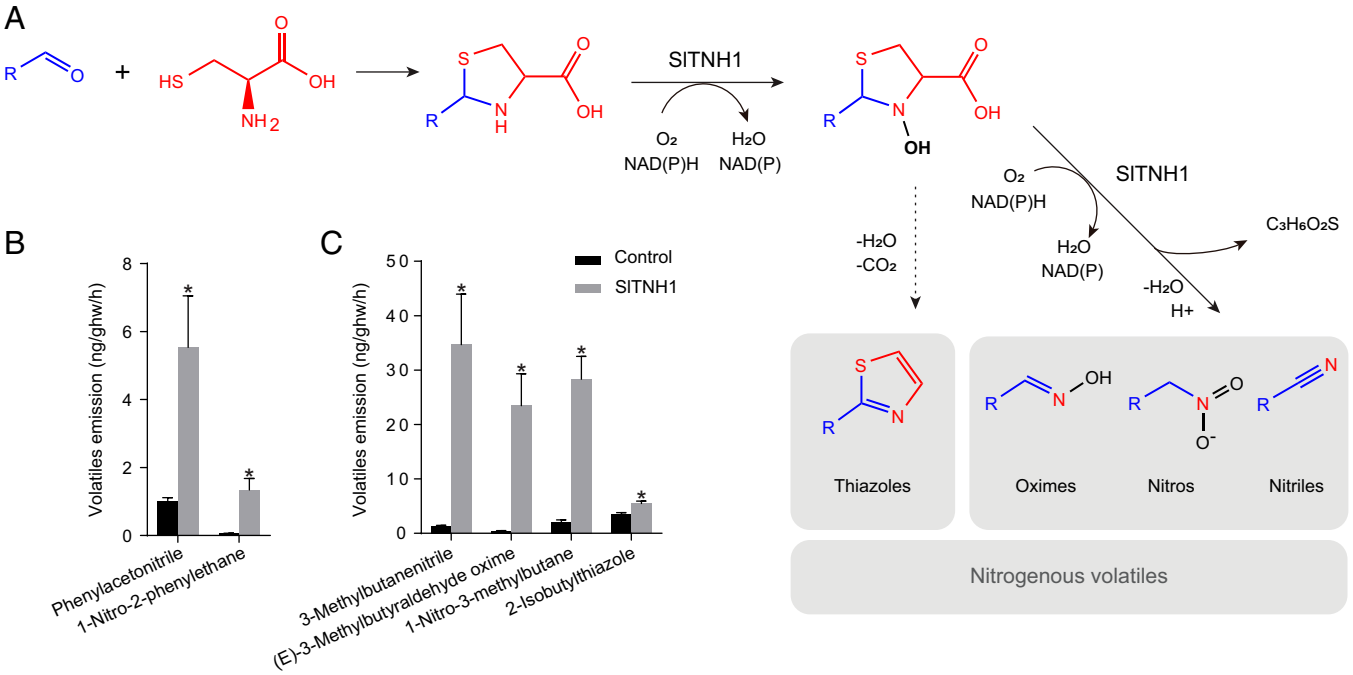

Fig. 6. Solyc12g013690 encodes a tetrahydrothiazolidine *N*-hydroxylase (TNH), and converts 2-tetrahydrothizolidines to nitrogenous flavor volatiles. (*A*) Model for TNH-dependent nitrogenous volatile biosynthesis in tomato fruit. (*B* and *C*) Nitrogenous flavor volatiles are produced in *N. benthamiana* leaves with transient expression of *SlTNH1* and supplementation with the corresponding thiazolidines made from 2-phenylacetaldehyde and L-cysteine (*B*), and 3-methylbutanal and L-cysteine (*C*). (±SE, $n = 4$, $^*P < 0.05$).

when provided 2-isobutyltetrahydrothiazolidine substrates derived from either L- or D-cysteine (Fig. 6 *A* and *C* and *SI Appendix*, Fig. S9). The 2-phenylacetaldehyde-derived tetrahydrothiazolidine substrate (*SI Appendix*, Fig. S10) was also readily transformed to 2-phenylacetonitrile and 1-nitro-2-phenylethane by *N. benthamiana* leaves expressing *Solyc12g013690* (Fig. 6*B*), identifying cysteine as the viable nitrogen source in these sulfur-free metabolites. Cysteamine-derived substrates lacking the 4-carboxyl group were not converted to volatiles (*SI Appendix*, Table S4). The volatile profiles generated by recombinant SlTNH1 in combination with 2-substituted tetrahydrothiazolidine substrates (Fig. 6 *A* and *B*) recapitulate the biosynthetic capacity of tomato fruit for nitrogenous volatile production (Figs. 1*B*, 2, and 3), and suggests that this enzyme catalyzes sequential *N*-hydroxylations. This conclusion is supported by UPLC-QTOF-MS analysis of these leaves that revealed detectable levels of a putative *N*-hydroxy-IT4C (*SI Appendix*, Fig. S11), consistent with the expected product of the first hydroxylation and a substrate for the second hydroxylation to generate volatiles (Fig. 6*A*). Therefore, we propose a new name for this enzyme: tetrahydrothiazolidine *N*-hydroxylase (TNH).

Discussion

Aroma is an important determinant of consumers' perception of and preference for fresh tomatoes. The nitrogenous volatiles are a set of simple, yet relatively unusual volatile compounds in plants, and are influential contributors to the complex mixture of tomato aroma. In contrast to tomato, the biosynthetic pathway to nitrogenous volatiles in poplar (*Populus trichocarpa*) relies on cytochrome P450-dependent enzymes (*SI Appendix*, Fig. S12). Herbivore-damaged poplar leaves produce nitrogenous volatiles such as 3-methylbutanenitrile, 2-methylbutanenitrile, 1-nitro-2-phenylethane, and 2-phenylacetonitrile. CYP79 family enzymes convert phenylalanine, leucine, and isoleucine to the corresponding aldoximes, which are subsequently converted to nitriles by a CYP71 family member (18, 43). The P450-dependent nitrile formation occurs in plants containing pathways for synthesis of cyanogenic glycosides (44, 45) and camalexin (46). Homologous CYP members in tomato are neither expressed highly in fruit nor in a ripening-associated manner according to RNA-sequencing data (47), suggesting other genes/enzymes are responsible for nitrogenous volatiles in tomato.

We set out to discover these unidentified biosynthetic genes in tomato using a QTL mapping approach, taking advantage of the differential accumulation of these aroma volatiles in fruits of *S. lycopersicum* versus *S. pennellii*. The top gene candidate, *Solyc12g013690*, was annotated as a FMO, a plausible catalyst for a biosynthetic pathway thought to proceed via oxidation of a primary amine (i.e., 3-methylbutylamine or 2-phenethylamine) (38, 48). Gene silencing experiments (Fig. 2) recapitulated the phenotypes of *S. pennellii* ILs with a strong reduction in all nitrogenous volatiles (*SI Appendix*, Table S1). Taken together, these results provide strong support for the essential role of *Solyc12g013690* in nitrogenous volatile biosynthesis. However, we did not observe any turnover of amine substrates in different heterologous expression and assay systems, suggesting different mechanisms and substrates beyond primary amines must be considered. A powerful and recognized approach in the functional elucidation of FMO enzymes (34, 49), we employed nontargeted metabolomics to identify metabolites affected by suppression of *Solyc12g013690* expression.

Complementary biosynthetic incorporation experiments using isotopically labeled cysteine, leucine, and phenylalanine revealed that cysteine, rather than a primary amine precursor derived from amino acid decarboxylation (i.e., phenethylamine), furnishes the N atom for nitrogenous volatile production in tomato (Fig. 5 and *SI Appendix*, Figs. S7 and S8). In contrast, Gonda et al. found that the same labeled phenylalanine fed to melon fruit resulted in the accumulation of isotopically labeled 2-phenylacetonitrile in both forms: nitrogen labeled (*m/z* 126) and unlabeled (*m/z* 125), with ^{13}C enrichment at all other atoms (21). Since the ubiquitous labeling of

2-phenylacetonitrile (*m/z* 126) observed was consistent with known (CYP79-based) mechanisms, the authors suggested that the lack of ^{15}N enrichment, the observation of labeled *m/z* 126, may indicate a second unknown mechanism in operation for nitrile formation in plants (21).

The current work demonstrates that another pathway for nitrogenous volatile formation does exist in plants, and this biosynthetic route is active in tomato fruit. Our data support a model for this pathway summarized in Fig. 6*A*. Cysteine levels increase in tomato fruit throughout development and ripening, reaching maximum levels in ripe tomato fruit (50–53). Concurrently, phenylalanine and leucine are being converted to aldehyde volatiles (*SI Appendix*, Table S1) (8, 12), providing favorable conditions for the spontaneous conjugation of aldehydes and cysteine to generate substituted thiazolidines. The formation of tetrahydrothiazolidines from cysteine and aldehydes is well documented (54) under mild, aqueous conditions, including thiazolidine formation in beer from cysteine and aldehydes (40). Expression of *SlTNH1* (*Solyc12g013690*) also increases throughout ripening (Fig. 3*B*), as does nitrogenous volatile production (Fig. 3*A*). These rising concentrations of tetrahydrothiazolidines are efficiently converted to a mixture of nitro, oximes, and nitriles via sequential *N*-hydroxylations by SlTNH1. Thiazoles are also produced following a single hydroxylation by SlTNH1 and subsequent dehydration and decarboxylation by an unknown mechanism.

FMOs can catalyze oxygenation of a wide range of substrates (35). In plants, they form a large group that is implicated in various biological functions, from defense against pathogens to synthesis of auxin and abscisic acid. Previous classification of plant enzymes focused on three clades (I, II, and III) belonging to group B (34). Clade I is represented by AtFMO1 that is associated with plant defense, which includes the recently characterized oxime synthase from ferns (55), while clade II contains enzymes implicated in the synthesis of glucosinolates (*At*GS-OX) (34). Clade III contains YUCCA and YUCCA-like enzymes and several members of that clade have been linked to the synthesis of auxin (56). Here we propose to extend the current classification to include plant FMOs belonging to additional clades (*SI Appendix*, Fig. S2). Clades IV and V include FMOs associated with zeaxanthin epoxidases and squalene epoxidases, respectively. Clade VII enzymes are homologous to the ubiquinone hydroxylase family (57), and clade VI includes SlTNH1. Proteins from clades IV to VII belong to group A or the closely related group E. Phylogenetically, plant groups A and E enzymes cluster together; but group E enzymes perform epoxidation reactions (35). Group E enzymes include zeaxanthin epoxidases (clade IV) that catalyze the conversion of zeaxanthin to violaxanthin as well as squalene epoxidases (clade V) that synthesize triterpenoid (35). Clade VI enzymes most likely belong to group A and are predicted to perform hydroxylation reactions. To our knowledge, no member of clade VI has a proven function. SlTNH1 therefore provides an important insight into that group.

The conversion of tetrahydrothiazolidines to dihydroxylated volatiles must result in the generation of a 3-sulfanylpropanoic acid (3-mercaptopropionic acid, 3-MPA) leaving group, or products thereof according to our evidenced-based model in Fig. 6*A*. Kiene and Taylor (58) first suggested that 3-MPA could be a central intermediate in organic sulfur metabolism; however, we were unable to detect 3-MPA in any of our samples. 3-MPA has long been recognized as a potent inhibitor of glutamate decarboxylase (59) via thiazolidine dead-end products (60). Since glutamate decarboxylase activity is undetectable in ripe tomato fruit (52) and plants are known to be sensitive to 3-MPA (61), we postulated that ripening-dependent 3-MPA production by SlTNH1 may be a biochemical mechanism to down-regulate GABA production, which is dependent on glutamate decarboxylase. However, tomatoes with differential SlTNH1 activity did not contain significantly different levels of GABA (*SI Appendix*, Fig. S13), reinforcing the notion that free 3-MPA does not accumulate as a product of SlTNH1 activity. At present, our hypothesis is that the 3-MPA moiety is broken down to H_2S and a C3 carboxylate by a mechanism analogous to cysteine desulfhydrases (62); however this putative route to H_2S is indiscriminant of cysteine stereochemistry, as both L- and D-cysteine are acceptable precursors (Fig. 6*C* and *SI Appendix*, Fig. S9).

In conclusion, we have demonstrated that a single flavin-monooxygenase type enzyme, TNH, is responsible for the biosynthesis of multiple aromatic and aliphatic nitrogen-containing volatile compounds in tomatoes and utilizes spontaneously formed cysteine conjugates as substrates. This pathway is distinct from the multistep pathway described in *Populus*. Thus plants have independently evolved at least two pathways for synthesis of these important volatiles.

Materials and Methods

Chemicals. All chemicals and standards were purchased from Sigma-Aldrich unless otherwise noted. The synthesis of tetrahydrothiazolidines was performed according to the procedure described by Ershov et al. (41). ^{1}H-NMR spectra were recorded on a Bruker AV 500-MHz spectrometer in D_2O or DMSO-d6 to confirm the structures of the products derived from 3-methylbutanal and cysteine (*SI Appendix*, Fig. S5) and 2-phenylacetaldehyde and cysteine (*SI Appendix*, Fig. S10). All adducts exhibited spectroscopic data in accord with the literature values.

Plant Materials and Treatments. Tomatoes (*S. lycopersicum*) were grown in a greenhouse or in the field at the University Laval (Quebec City, QC, Canada) or at Live Oak, FL. Seeds of the original ILs were provided by D. Zamir (28). For the ethylene and 1-MCP treatments, cv. Pearson and the isogenic *Never-ripe* mutant were used. The treatments were performed as previously described (63). Briefly, ethylene treatment was applied at a final concentration of 50 $\mu L \cdot L^{-1}$ in a sealed 20-L container at 20° for 16 h. A total of 2 $\mu L \cdot L^{-1}$ 1-MCP was generated by adding 0.055 g 1-MCP powder (SmartFresh Quality System, 0.14% active ingredient, AgroFresh, Inc., Rohm and Haas) to a flask containing 25 mL of distilled water in a sealed 20-L container. The 1-MCP treatment was done for 12 h at 20 °C.

Fine Mapping. New recombinants were obtained from a cross between *S. lycopersicum* cv. M82 and IL12-2. The genome organization of these smaller introgression lines was determined by a set of CAPS and INDEL molecular markers developed by comparing the available genome sequence of *S. lycopersicum* and *S. pennellii* (64, 65). The phenotype for each line was assessed by volatile collection as described below.

Collection and Analysis of Aroma Volatiles. Volatiles were collected from ~100 g chopped ripe fruits for 1 h in a glass tube (inner diameter 2.5 cm × length 60 cm) with a flow of activated carbon filtered air. Volatiles were trapped on a divinylbenzene resin column (HayeSep Q, 80 to 100 mesh size) and eluted with methylene chloride using nonyl acetate as an internal control. Samples were separated on a DB-5 column (30 m, 1-μM film thickness, 0.25 mm inner diameter (ID); Agilent) and analyzed on an Agilent 7890B gas chromatograph with flame ionization detection using hydrogen as a carrier gas (1 $mL \cdot min^{-1}$). The gas chromatography (GC) oven temperature was 35 °C (hold for 1 min) and increased up to 250 °C (6 $°C \cdot min^{-1}$). Quantification was performed by calculating the peak area and comparing it to the internal standard nonyl acetate. Peaks were identified by comparing to the retention times of known standards and furthermore confirmed by GC/MS (Agilent 5977 MS) using a DB-5MS column and helium as a carrier gas. The GC-MS oven temperature was going from 35 °C (hold for 1.5 min) to 47 °C (6 $°C \cdot min^{-1}$) and then to 250 °C (10 $°C \cdot min^{-1}$). Statistical analyses were performed by one-way analysis of variance (ANOVA) followed by a Tukey multiple comparison test. Volatiles content is expressed as nanograms emitted per gram of fresh weight per hour.

Metabolite Profiling by UPLC-QTOF-MS. Chopped, ripe tomato fruits or fresh *N. benthamiana* leaves were flash-frozen in liquid nitrogen, freeze-dried, and ground to a fine powder and stored at −80 °C until extraction. Approximately 40 mg of powdered tissue was extracted with 1 mL of 75:25 methanol/water, acidified with 0.1% formic acid, and sonicated 2 × 15 min after vortexing briefly. The extracts were centrifuged for 15 min at 15,000 × *g* and filtered

through 0.2-μm GHP syringe filters (Waters). Extracts were analyzed in electrospray ionization positive (ESI +) mode on a Waters Acquity I-Class UPLC coupled to a Waters Xevo G2-XS QTOF mass spectrometer. Relatively semipolar metabolites were analyzed on a BEH C18 column (Waters) according to Rogachev and Aharoni (66). Polar metabolites (3-MPA, GABA) were analyzed using a BEH Amide column (Waters) and according to Gika et al. (67). Peak alignment, quality-control assessment, peak picking, pseudomolecular ion (adduct) composition, and normalization to all mass features were performed in Progenesis QI (nonlinear dynamics) and multivariate statistical analyses (principal component analysis, OPLS-DA) were performed using Progenesis QI and EzInfo. Raw data of features of interest were assessed using MassLynx.

Atmospheric Pressure GC-MS. To evaluate the biosynthetic incorporation of stable-isotope–labeled amino acids into nitrogenous volatiles including 2-isobutylthiazole and 2-phenylacetonitrile, a volatile extraction and APGC-QTOF-MS experiment was conducted on tomatoes injected with 5 mM L-Cys, 5 mM ^{15}N,$^{13}C_3$-L-Cys, 5 mM $^{13}C_9$, ^{15}N-phenylalanine, or distilled water. Volatile collection was performed as described above.

To improve detection sensitivity of the APGC-QTOF analysis to detect $^{13}C_8$-2-phenylacetonitrile, the corona pin position was first optimized for detecting a 2-phenylacetonitrile standard. A corona pin position of 1.5 to 2.0 mm from the center point of the sample cone orifice with current of 1.5 μA was determined to be optimal. APGC-MS analysis of tomato volatiles was performed using a 7890 GC system (Agilent Technologies Inc.) coupled to a Xevo G2-XS QTOF mass spectrometer (Waters Corporation). A 7693A automatic liquid sampler (Agilent) was used to inject a 5-μL volume of volatile extract onto the GC with an inlet temperature of 280 °C in splitless mode. Chromatographic separation was performed using a DB-5MS column (length 30 m × 0.250 mm ID × film thickness 0.25 μm; Agilent). Carrier gas flow (helium) was 2.0 mL·min^{-1} with a constant flow inlet mode, make-up flow (nitrogen) was 250 mL·min^{-1}, auxiliary gas flow (nitrogen) was 100 L·h^{-1}, and cone gas flow (nitrogen) was 140 L·h^{-1}. The column oven ramp was as follows: 40 °C (hold for 1 min), 50 °C·min^{-1} ramp to a maximum temperature of 280 °C (1 min hold at maximum temperature). The transfer line temperature was 310 °C. A mass range of 50 to 300 Da was collected in atmospheric pressure ionization positive (API +) mode for a total acquisition time of 6.8 min. Accurate mass measurements were lockmass corrected using background column bleed ions (281.0517 Da). Instrument operation and data management were conducted using Waters MassLynx software.

Transgenic Plants and EMS Variant. The full-length *SlTNH1* was cloned into the plasmid pHKAS (68) in the antisense orientation. *S. lycopersicum* cv. Large Red Cherry cotyledons were transformed with *Agrobacterium tumefaciens* strain ABI as described (69) using kanamycin as a selective agent. Volatiles from the fruits of transgenic plants were collected as described above. Phenotypes were heritable across multiple generations and the analysis was done on the T3 generation.

The TNH1 W278stop variant line was isolated from an EMS-mutagenized tomato population in Vendor background via a reverse genetics method called deep variant scanning (DVS) (70). The DVS method identifies tomato lines harboring single nucleotide polymorphisms (SNPs) in the target gene (in this case aroma-related genes) using a high-resolution DNA melt curve analysis approach. The *SlTNH1* gene was amplified by PCR from pooled DNA samples representing mutagenized M2 plants from a tomato population. Amplicons representing multiple genes were pooled stoichiometrically and prepared for high-throughput Illumina sequencing with a Nextera XT kit. The DVS bioinformatics pipeline was used to call likely SNPs (i.e., mutations) relative to the wild-type sequence. Putative mutations were confirmed and assigned to an individual M2 family by high-resolution DNA melting. Seeds of the variant tomato lines (M2) harboring the desired genetic variations were sown in 72-cell flats in soil and the resulting seedlings genotyped with respect to the SNP of interest to determine whether they are homozygous or heterozygous for the variant allele (aa), or if they are wild-type segregants (AA). At least three individuals of each genotype were transplanted to soil in 1-gallon pots or to a hydroponic system and cultivated under standard greenhouse production conditions to yield red, ripe fruit. Heterozygotes were backcrossed to the recurrent parent, Vendor or to elite inbred lines, and progeny were subsequently selfed to generate homozygous variants segregating in the F_2.

Transient Expression in *N. benthamiana*. Six-week-old plants (~25 g) were vacuum infiltrated with *A. tumefaciens* harboring the plasmid pBIN61 with the silencing suppressor p19 (71) (control) or a mixture of pBIN61-p19 and pHKOE with the full-length sequence of SlTNH1 (optical density ~0.4, 10 mM $MgCl_2$, 10 mM 2-morpholinoethanesulfonic acid (MES) pH 5.6). After 4 d in a growth chamber at 20 °C (16 h light), the four youngest fully developed agroinfiltrated leaves per plant were infiltrated with a 10-mM solution of 2-tetrahydrothizolidines derived from an aldehyde (3-methylbutanal, phenylacetaldehyde) and cysteine (L or D). The 2-benzyl-1,3-thiazolidine-4-carboxylic acid is slightly soluble at room temperature and tends to precipitate over time, while 2-isobutyl-1,3-thiazolidine-4-carboxylic acid is readily soluble in water. After 24 h, the leaves were harvested (10 g) and analyzed as described above.

RNA Extraction and Quantitative PCR. Total RNA was extracted from the fruit tissues used for volatile analyses. Possible genomic DNA contamination was removed by DNase treatment. Quantitative PCR was performed using Power SYBR Green RNA-to-C_T 1-Step kit (Applied Biosystems). The following set of primers: 5′-TGCTACTTCTTTGGCCCTTC-3′ and 5′-TCTCCAGGCATTAGTCCACA-3′, was used to quantify *SlTNH1* in the introgression lines using a standard curve of a purified plasmid containing the coding sequence. To validate the expression level in transgenic plants, a fragment starting in the 5′ untranslated region of *SlTNH1* was amplified with the following set of primers: 5′-GGGAGAAACAGAGAAATAATGGAG-3′ and 5′-CAGTAGCTCGCAACGAATCA-3′. Copy numbers of transcripts were determined using a standard curve made from amplified fragments obtained by PCR with the same primers. Statistical analyses were performed by ANOVA followed by a Tukey multiple comparison test.

Sequence and Phylogenetic Analysis. Multiple sequence alignment and homology analysis of the DNA and protein sequences was performed using MAFFT (72). The phylogenetic tree was built using MEGA6 (73). The tree was inferred by using the maximum likelihood method with 1,000 bootstrap replicates. The initial tree for the heuristic search was obtained automatically by applying neighbor-joining and BioNJ algorithms to a matrix of pairwise distances estimated using the Jones–Thornton–Taylor (JTT) model and then selecting the topology with superior log likelihood value. All positions with less than 75% site coverage were eliminated.

Data Availability. All study data are included in the article and/or *SI Appendix*.

ACKNOWLEDGMENTS. This work was supported by funding from Genome Canada (C.G. and D.K.L.), the Ontario Ministry of Research and Innovation (D.K.L.), Growing Forward 2, Ontario Greenhouse Vegetable Growers (D.K.L.), Genome Quebec (C.G.), the Canada Foundation for Innovation (C.G. and D.K.L.), and in part by grants from the NSF (IOS-0923312 to H.J.K.) and the Natural Sciences and Engineering Research Council of Canada (NSERC) (to C.G.). C.J.K. is the recipient of a Canada Graduate Doctoral Scholarship from NSERC. We thank Dawn Bies, Mark Taylor, and Dr. Miguel Botella for their technical assistance and helpful discussions, as well as Dr. Jon Stewart and Dr. Andrew Hanson for their valuable insights into FMO enzyme chemistry.

1. Y. Bai, P. Lindhout, Domestication and breeding of tomatoes: What have we gained and what can we gain in the future? *Ann. Bot.* **100**, 1085–1094 (2007).
2. D. Tieman *et al.*, A chemical genetic roadmap to improved tomato flavor. *Science* **355**, 391–394 (2017).
3. H. J. Klee, Improving the flavor of fresh fruits: Genomics, biochemistry, and biotechnology. *New Phytol.* **187**, 44–56 (2010).
4. E. A. Baldwin, K. Goodner, A. Plotto, Interaction of volatiles, sugars, and acids on perception of tomato aroma and flavor descriptors. *J. Food Sci.* **73**, S294–S307 (2008).
5. D. Tieman *et al.*, The chemical interactions underlying tomato flavor preferences. *Curr. Biol.* **22**, 1035–1039 (2012).
6. S. A. Goff, H. J. Klee, Plant volatile compounds: Sensory cues for health and nutritional value? *Science* **311**, 815–819 (2006).
7. D. Tieman *et al.*, Tomato aromatic amino acid decarboxylases participate in synthesis of the flavor volatiles 2-phenylethanol and 2-phenylacetaldehyde. *Proc. Natl. Acad. Sci. U.S.A.* **103**, 8287–8292 (2006).
8. A. Kochevenko *et al.*, Catabolism of branched chain amino acids supports respiration but not volatile synthesis in tomato fruits. *Mol. Plant* **5**, 366–375 (2012).
9. A. Clavijo McCormick, S. B. Unsicker, J. Gershenzon, The specificity of herbivore-induced plant volatiles in attracting herbivore enemies. *Trends Plant Sci.* **17**, 303–310 (2012).
10. D. Lucas-Barbosa, J. J. van Loon, M. Dicke, The effects of herbivore-induced plant volatiles on interactions between plants and flower-visiting insects. *Phytochemistry* **72**, 1647–1654 (2011).
11. H. J. Klee, J. J. Giovannoni, Genetics and control of tomato fruit ripening and quality attributes. *Annu. Rev. Genet.* **45**, 41–59 (2011).
12. D. M. Tieman *et al.*, Identification of loci affecting flavour volatile emissions in tomato fruits. *J. Exp. Bot.* **57**, 887–896 (2006).
13. J. Takabayashi, S. Takahashi, M. Dicke, M. A. Posthumus, Developmental stage of herbivore *Pseudaletia separata* affects production of herbivore-induced synomone by corn plants. *J. Chem. Ecol.* **21**, 273–287 (1995).
14. C. E. van den Boom, T. A. van Beek, M. A. Posthumus, A. de Groot, M. Dicke, Qualitative and quantitative variation among volatile profiles induced by *Tetranychus urticae* feeding on plants from various families. *J. Chem. Ecol.* **30**, 69–89 (2004).

15. A. Zhang, J. S. Hartung, Phenylacetaldehyde O-methyloxime: A volatile compound produced by grapefruit leaves infected with the citrus canker pathogen, *Xanthomonas axonopodis* pv. citri. *J. Agric. Food Chem.* **53**, 5134–5137 (2005).
16. K. Noge, M. Abe, S. Tamogami, Phenylacetonitrile from the giant knotweed, *Fallopia sachalinensis*, infested by the Japanese beetle, *Popillia japonica*, is induced by exogenous methyl jasmonate. *Molecules* **16**, 6481–6488 (2011).
17. A. Clavijo McCormick *et al.*, Herbivore-induced volatile emission in black poplar: Regulation and role in attracting herbivore enemies. *Plant Cell Environ.* **37**, 1909–1923 (2014).
18. S. Irmisch *et al.*, Two herbivore-induced cytochrome P450 enzymes CYP79D6 and CYP79D7 catalyze the formation of volatile aldoximes involved in poplar defense. *Plant Cell* **25**, 4737–4754 (2013).
19. R. Buttery, "Quantitative and sensory aspects of flavor of tomato and other vegertables and fruits" in *Flavor Science: Sensible Principles and Techniques*, T. E. Acree, R. Teranishi, Eds. (American Chemical Society, 1993), pp. 259–286.
20. E. A. Baldwin, J. W. Scott, C. K. Shewmaker, W. Schuch, Flavor trivia and tomato aroma: Biochemistry and possible mechanisms for control of important aroma components. *HortScience* **35**, 1013–1022 (2000).
21. I. Gonda *et al.*, Differential metabolism of L-phenylalanine in the formation of aromatic volatiles in melon (*Cucumis melo* L.) fruit. *Phytochemistry* **148**, 122–131 (2018).
22. R. Kaiser, L. Tollsten, An introduction to the scent of cacti. *Flavour Fragr. J.* **10**, 153–164 (1995).
23. R. Kaiser, Vanishing flora–lost chemistry: The scents of endangered plants around the world. *Chem. Biodivers.* **1**, 13–27 (2004).
24. G. P. Svensson, T. Okamoto, A. Kawakita, R. Goto, M. Kato, Chemical ecology of obligate pollination mutualisms: Testing the 'private channel' hypothesis in the *Breynia-Epicephala* association. *New Phytol.* **186**, 995–1004 (2010).
25. Y. Kuwahara, Y. Ichiki, M. Morita, Y. Asano, (2-Nitroethyl)benzene: A major flower scent from the Japanese loquat *Eriobotrya japonica* [Rosales: Rosaceae]. *Biosci. Biotechnol. Biochem.* **78**, 1320–1323 (2014).
26. B. Hamberger, S. Bak, Plant P450s as versatile drivers for evolution of species-specific chemical diversity. *Philos. Trans. R. Soc. Lond. B Biol. Sci.* **368**, 20120426 (2013).
27. S. Mathieu *et al.*, Flavour compounds in tomato fruits: Identification of loci and potential pathways affecting volatile composition. *J. Exp. Bot.* **60**, 325–337 (2009).
28. Y. Eshed, D. Zamir, An introgression line population of *Lycopersicon pennellii* in the cultivated tomato enables the identification and fine mapping of yield-associated QTL. *Genetics* **141**, 1147–1162 (1995).
29. C. Goulet *et al.*, Role of an esterase in flavor volatile variation within the tomato clade. *Proc. Natl. Acad. Sci. U.S.A.* **109**, 19009–19014 (2012).
30. C. Goulet *et al.*, Divergence in the enzymatic activities of a tomato and *Solanum pennellii* alcohol acyltransferase impacts fruit volatile ester composition. *Mol. Plant* **8**, 153–162 (2015).
31. Y. M. Tikunov *et al.*, The genetic and functional analysis of flavor in commercial tomato: The FLORAL4 gene underlies a QTL for floral aroma volatiles in tomato fruit. *Plant J.* **103**, 1189–1204 (2020).
32. M. B. Lanahan, H. C. Yen, J. J. Giovannoni, H. J. Klee, The never ripe mutation blocks ethylene perception in tomato. *Plant Cell* **6**, 521–530 (1994).
33. E. C. Sisler, M. Serek, Inhibitors of ethylene responses in plants at the receptor level: Recent developments. *Physiol. Plant.* **100**, 577–582 (1997).
34. N. L. Schlaich, Flavin-containing monooxygenases in plants: Looking beyond detox. *Trends Plant Sci.* **12**, 412–418 (2007).
35. M. M. Huijbers, S. Montersino, A. H. Westphal, D. Tischler, W. J. van Berkel, Flavin dependent monooxygenases. *Arch. Biochem. Biophys.* **544**, 2–17 (2014).
36. R. K. Wierenga, P. Terpstra, W. G. Hol, Prediction of the occurrence of the ADP-binding $\beta\,\alpha\,\beta$-fold in proteins, using an amino acid sequence fingerprint. *J. Mol. Biol.* **187**, 101–107 (1986).
37. G. Eggink, H. Engel, G. Vriend, P. Terpstra, B. Witholt, Rubredoxin reductase of *Pseudomonas oleovorans*. Structural relationship to other flavoprotein oxidoreductases based on one NAD and two FAD fingerprints. *J. Mol. Biol.* **212**, 135–142 (1990).
38. H. J. Klee, D. M. Tieman, The genetics of fruit flavour preferences. *Nat. Rev. Genet.* **19**, 347–356 (2018).
39. D. N. Crowell *et al.*, *Arabidopsis thaliana* plants possess a specific farnesylcysteine lyase that is involved in detoxification and recycling of farnesylcysteine. *Plant J.* **50**, 839–847 (2007).
40. J. J. Baert, J. De Clippeleer, L. De Cooman, G. Aerts, Exploring the binding behavior of beer staling aldehydes in model systems. *J. Am. Soc. Brew. Chem.* **73**, 100–108 (2015).
41. A. Y. Ershov, D. G. Nasledov, I. V. Lagoda, V. V. Shamanin, Synthesis of 2-substituted (2R, 4R)-3-(3-mercapto-propionyl) thiazolidine-4-carboxylic acids. *Chem. Heterocycl. Compd.* **50**, 1032–1038 (2014).
42. F. Geu-Flores *et al.*, Cytosolic γ-glutamyl peptidases process glutathione conjugates in the biosynthesis of glucosinolates and camalexin in Arabidopsis. *Plant Cell* **23**, 2456–2469 (2011).
43. S. Irmisch *et al.*, Herbivore-induced poplar cytochrome P450 enzymes of the CYP71 family convert aldoximes to nitriles which repel a generalist caterpillar. *Plant J.* **80**, 1095–1107 (2014).
44. S. Bak, R. A. Kahn, H. L. Nielsen, B. L. Møller, B. A. Halkier, Cloning of three A-type cytochromes P450, CYP71E1, CYP98, and CYP99 from *Sorghum bicolor* (L.) Moench by a PCR approach and identification by expression in *Escherichia coli* of CYP71E1 as a multifunctional cytochrome P450 in the biosynthesis of the cyanogenic glucoside dhurrin. *Plant Mol. Biol.* **36**, 393–405 (1998).
45. A. M. Takos *et al.*, Genomic clustering of cyanogenic glucoside biosynthetic genes aids their identification in *Lotus japonicus* and suggests the repeated evolution of this chemical defence pathway. *Plant J.* **68**, 273–286 (2011).
46. M. Nafisi *et al.*, Arabidopsis cytochrome P450 monooxygenase 71A13 catalyzes the conversion of indole-3-acetaldoxime in camalexin synthesis. *Plant Cell* **19**, 2039–2052 (2007).
47. Tomato Genome Consortium, The tomato genome sequence provides insights into fleshy fruit evolution. *Nature* **485**, 635–641 (2012).
48. M. Hartmann *et al.*, Flavin monooxygenase-generated N-hydroxypipecolic acid is a critical element of plant systemic immunity. *Cell* **173**, 456–469 (2018).
49. S. Thodberg, E. H. Jakobsen Neilson, The "Green" FMOs: Diversity, functionality and application of plant flavoproteins. *Catalysts* **10**, 329 (2020).
50. Y. Fuchs, E. Pesis, G. Zauberman, L. Tabachnik, Free sulfhydryl groups in ripening tomato fruits. *Plant Cell Physiol.* **22**, 733–736 (1981).
51. L. Tabachnik-Ma'ayan, Y. Fuchs, Free sulfhydryl groups in ripening fruits. *Plant Cell Physiol.* **23**, 1309–1314 (1982).
52. S. B. Boggio, J. F. Palatnik, H. W. Heldt, E. M. Valle, Changes in amino acid composition and nitrogen metabolizing enzymes in ripening fruits of *Lycopersicon esculentum* Mill. *Plant Sci.* **159**, 125–133 (2000).
53. F. Carrari *et al.*, Integrated analysis of metabolite and transcript levels reveals the metabolic shifts that underlie tomato fruit development and highlight regulatory aspects of metabolic network behavior. *Plant Physiol.* **142**, 1380–1396 (2006).
54. H. Soloway, F. Kipnis, J. Ornfelt, P. E. Spoerri, 2-Substituted-thiazolidine-4-carboxylic Acids. *J. Am. Chem. Soc.* **70**, 1667–1668 (1948).
55. S. Thodberg *et al.*, A flavin-dependent monooxygenase catalyzes the initial step in cyanogenic glycoside synthesis in ferns. *Commun. Biol.* **3**, 1–11 (2020).
56. N. D. Tivendale, J. J. Ross, J. D. Cohen, The shifting paradigms of auxin biosynthesis. *Trends Plant Sci.* **19**, 44–51 (2014).
57. K. Hayashi *et al.*, Functional conservation of coenzyme Q biosynthetic genes among yeasts, plants, and humans. *PLoS One* **9**, e99038 (2014).
58. R. P. Kiene, B. F. Taylor, Biotransformations of organosulphur compounds in sediments via 3-mercaptopropionate. *Nature* **332**, 148–150 (1988).
59. C. Lamar Jr., Mercaptopropionic acid: A convulsant that inhibits glutamate decarboxylase. *J. Neurochem.* **17**, 165–170 (1970).
60. P. Liu, M. P. Torrens-Spence, H. Ding, B. M. Christensen, J. Li, Mechanism of cysteine-dependent inactivation of aspartate/glutamate/cysteine sulfinic acid α-decarboxylases. *Amino Acids* **44**, 391–404 (2013).
61. Y. Ling *et al.*, γ-Aminobutyric acid (GABA) homeostasis regulates pollen germination and polarized growth in *Picea wilsonii*. *Planta* **238**, 831–843 (2013).
62. J. Papenbrock, A. Riemenschneider, A. Kamp, H. N. Schulz-Vogt, A. Schmidt, Characterization of cysteine-degrading and H2S-releasing enzymes of higher plants - From the field to the test tube and back. *Plant Biol.* **9**, 582–588 (2007).
63. Y. Kamiyoshihara, D. M. Tieman, D. J. Huber, H. J. Klee, Ligand-induced alterations in the phosphorylation state of ethylene receptors in tomato fruit. *Plant Physiol.* **160**, 488–497 (2012).
64. N. Fernandez-Pozo *et al.*, The sol genomics network (SGN) - From genotype to phenotype to breeding. *Nucleic Acids Res.* **43**, D1036–D1041 (2015).
65. A. Bolger *et al.*, The genome of the stress-tolerant wild tomato species *Solanum pennellii*. *Nat. Genet.* **46**, 1034–1038 (2014).
66. I. Rogachev, A. Aharoni, UPLC-MS-based metabolite analysis in tomato. *Methods Mol. Biol.* **860**, 129–144 (2012).
67. H. G. Gika, G. A. Theodoridis, U. Vrhovsek, F. Mattivi, Quantitative profiling of polar primary metabolites using hydrophilic interaction ultrahigh performance liquid chromatography-tandem mass spectrometry. *J. Chromatogr. A* **1259**, 121–127 (2012).
68. A. J. Simkin *et al.*, Circadian regulation of the PhCCD1 carotenoid cleavage dioxygenase controls emission of β-ionone, a fragrance volatile of petunia flowers. *Plant Physiol.* **136**, 3504–3514 (2004).
69. H. J. Sun, S. Uchii, S. Watanabe, H. Ezura, A highly efficient transformation protocol for Micro-Tom, a model cultivar for tomato functional genomics. *Plant Cell Physiol.* **47**, 426–431 (2006).
70. T. Banks, D. Somers, High throughput method of screening a population for members comprising mutations(s) in a target sequence using alignment-free sequence analysis. CA patent 2911002 (2016).
71. D. Baulcombe, RNA silencing in plants. *Nature* **431**, 356–363 (2004).
72. K. Katoh, K. Misawa, K. Kuma, T. Miyata, MAFFT: A novel method for rapid multiple sequence alignment based on fast Fourier transform. *Nucleic Acids Res.* **30**, 3059–3066 (2002).
73. K. Tamura, G. Stecher, D. Peterson, A. Filipski, S. Kumar, MEGA6: Molecular evolutionary genetics analysis version 6.0. *Mol. Biol. Evol.* **30**, 2725–2729 (2013).